Sequence characterization of eccDNA content in glyphosate sensitive and resistant Palmer amaranth from geographically distant populations

Hailey Spier Camposano[1], William T. Molin[2], and Christopher A. Saski[1]*

[1]Department of Plant and Environmental Sciences, Clemson University, Clemson SC, USA

[2]Crop Production Systems Research Unit, United States Department of Agriculture, Stoneville, MS, USA

*Corresponding author

E-mail: saski@clemson.edu (CU)

Abstract

The discovery of non-chromosomal circular DNA offers new directions in linking genome structure with function in plant biology. Glyphosate resistance through *EPSPS* gene copy amplification in Palmer amaranth was due to an autonomously replicating extra-chromosomal circular DNA mechanism (eccDNA). CIDER-Seq analysis of geographically distant glyphosate sensitive (GS) and resistant (GR) Palmer Amaranth (*Amaranthus palmeri*) revealed the presence of numerous small extra-chromosomal circular DNAs varying in size and with degrees of repetitive content, coding sequence, and motifs associated with autonomous replication. In GS biotypes, only a small portion of these aligned to the 399 kb eccDNA replicon, the vehicle underlying gene amplification and genetic resistance to the herbicide glyphosate. The aligned eccDNAs from GS were separated from one another by large gaps in sequence. In GR biotypes, the eccDNAs were present in both abundance and diversity to assemble into a nearly complete eccDNA replicon. Mean sizes of eccDNAs were similar in both biotypes and were around 5kb with larger eccDNAs near 25kb. Gene content for eccDNAs ranged from 0 to 3 with functions that include ribosomal proteins, transport, metabolism, and general stress response genetic elements. Repeat content among smaller eccDNAs indicate a potential for recombination into larger structures. Genomic hotspots were also identified in the Palmer amaranth genome with a disposition for gene focal amplifications as eccDNA. The presence of eccDNA may serve as a reservoir of genetic heterogeneity in this species and may be functionally important for survival.

Introduction

Extra-chromosomal circular DNA (eccDNA) are nucleus limited ring-like DNA entities derived from the genome and have been found in a wide range of eukaryotic organisms including yeast, *Drosophila*, *Xenopus*, mice, and humans [1-4]. In yeast, eccDNAs with functional genes and sizes of up to 38 kb that cover 23% of the genome have been reported [5]. EccDNAs have been reported in normal healthy cells in humans [6, 7] with functions associated with aging and the formation of telomeric circles [8, 9], cancer progression, and therapeutic resistance [10-12]. EccDNAs have been implicated in approximately half of all human cancers contributing to genetic heterogeneity that enables aggressive tumors with a selective advantage; hence the higher prevalence in malignant tumors [13-15]. Sizes of cancer related eccDNA have been reported to range from several hundred base pairs to 600 kb encoded with functional oncogenes and their various regulatory elements [16, 17]. In plants, eccDNAs have been reported in *Arabidopsis* [18, 19], *Oryza*, *Pisum*, *Secale*, *Triticum*, and *Vicia* [20, 21] with sizes that range from 1 kb to 50kb. These eccDNAs contain coding sequences commonly found within the nucleus such as ribosomal genes, tRNAs, and transposons [19, 22, 23]. EccDNAs are thought to arise from linear chromosomes through repeat-mediated intrachromosomal homologous recombination that results in the 'looping-out' of circular structures. These focal amplifications are mediated by multimers corresponding to 5S ribosomal DNA, non-coding chromosomal high-copy tandem repeats, and telomeric DNA [1, 21, 22]. In *Arabidopsis*, eccDNA genesis is the result of recombination among inverted repeats upstream and downstream of the various tRNAs and transposons [19]. Several follow up studies using *Arabidopsis* and

rice, have shown that defective RNA polymerase II (Pol II) activity and simultaneous inhibition of DNA methylation leads to the activation of retrotransposons which can induce eccDNA formation upon stress [11]. These studies suggest a possible relationship among epigenetic status, regulation of transposon bursts, and genomic focal amplifications.

The presence of eccDNA with functional genes in a cell can be a signature of a stress and/or function as a reservoir of genetic variation in which a cell may activate as a rapid response to stress. For example, oncogene amplification and expression via eccDNA in human cancers provides a unique mechanism for massive gene expression [24] and ultimately a reservoir of genetic heterogeneity by which cancer cells have a selective advantage for aggressive behavior and persistence [13].

Recently, the genetic entity conferring resistance to the herbicide glyphosate in Palmer amaranth (*Amaranthus palmeri*), now termed the eccDNA replicon, was revealed to be a massive, 399 kb extrachromosomal circular DNA (eccDNA) [25, 26]. Glyphosate resistance in Palmer amaranth is achieved through replicon amplification with simultaneous gene copy amplification and expression of the 5-enoylpyruvylshikimate-3-phosphate synthase (*EPSPS*) gene and its product, EPSP synthase [27], which is the herbicide target of glyphosate [28]. Glyphosate resistance may occur with as few as 5 copies of *EPSPS.* The increase in *EPSPS* functions to ameliorate the unbalanced or unregulated metabolic changes, such as shikimate accumulation, loss of aromatic amino acids, phenolic acids for lignin synthesis, and structural intermediates for plant growth regulators associated with glyphosate activity in sensitive plants [27, 29]. Isolation and single-molecule sequencing of the replicon

resulted in a single copy of the *EPSPS* gene along with 58 other predicted genes whose broad functions traverse detoxification, replication, recombination, DNA binding, and transport [26, 30]. Gene expression profiling of the replicon under glyphosate treatment showed transcription of 41 of the 59 genes in GR biotypes, with high expression of *EPSPS*, aminotransferase, zinc-finger, and several uncharacterized proteins [26, 30].

Repeat sequences and mobile genetic elements have been associated with eccDNA formation [4, 6, 18, 20, 30, 31] in higher eukaryotes. The repeat landscape of the replicon is described as a complex arrangement of repeat sequences and mobile genetic elements interspersed among arrays of clustered palindromes which may function in stability, DNA duplication and/or a means of nuclear integration [26]. In a follow up study, sequence analysis identified a region in the replicon with elevated A+T content and an exact match to a conserved eukaryotic extended autonomous consensus sequence (EACS) [32]. Surrounding this sequence were multiple DNA unwinding elements (DUE), which together are often associated with DNA bending and origins of replication and typically found near EACS [33, 34]. Regions flanking these elements in the replicon were cloned into an ARS-less yeast plasmid which resulted in colony formation, suggesting autonomous replication as the mechanism for the replicon increases in copy number [35].

Initial low-resolution FISH analysis of GR *A. palmeri* showed the amplified *EPSPS* gene was randomly distributed in the genome, suggesting a possible transposon-based mechanism of mobility [27]. A follow up study using much longer bacterial artificial chromosome (BAC) probes coupled with high resolution fiber extension microscopy verified the eccDNA replicon and identified various structural

105 polymorphisms including intact, circular, dimerized circular, and linear forms [25].
106 Additionally, this study resolved a critical question regarding the maintenance
107 mechanism that explains uneven segregation of glyphosate resistance among
108 progenies – genomic tethering. Analysis of fiber-FISH images with replicon probes and
109 meiotic pachytene chromosomes revealed very clear, single signals [25]. If the replicon
110 were integrated into the genome, then double signals would be evident, suggesting a
111 tethering mechanism as a means of genomic persistence to daughter cells during cell
112 division [25]. Other genetic entities that maintain genomic persistence through tethering
113 include DNA viruses such as Epstein-Barr, Rhadinovirus, Papillomavirus, and others
114 [36].

115 Glyphosate resistance in Palmer amaranth has been observed in individuals with
116 *EPSPS* copy numbers that range from 5-150 copies [27, 37, 38]. Amplification of the
117 *EPSPS* gene correlated with amplification of flanking genes and sequence [26, 30],
118 which suggests a large amplification unit and genome size enlargement in cells with
119 many replicon copies [30]. Flow cytometry verified significant genome expansion in
120 plants with high copy numbers (eg. 11% increase in genome size with ~100 extra
121 copies of the replicon), seemingly without fitness penalty [30].

122 Glyphosate resistance in Palmer amaranth was originally reported in Georgia in
123 the early 2,000's [39], and a recent analysis using whole genome shotgun sequencing
124 verified that the replicon was present and intact in GR Palmer amaranth populations
125 across the USA [40, 41]. This study also reported a lack of replicon SNP variation
126 among GR eccDNAs from geographically distant states when aligned to the Mississippi
127 replicon reference [26]. The replicon was not present in GS individuals, which supports

a single origin hypothesis and spread of the replicon across the USA through mechanical means such as spread of GR pollen in contaminated plant products, on farm equipment, and cattle movement, or via pollen.

The genomic mechanisms, origins and how the replicon assembled and gave rise to eccDNA in Palmer amaranth remains elusive, but the above studies lead to a couple of hypotheses: 1) the eccDNA replicon formed through intramolecular recombination among distal parts of the nuclear genome in short evolutionary time, or 2) there may exist a reservoir of smaller eccDNAs that are basal in the cell that may have the ability to recombine to assemble larger units as part of a dynamic response to stress. In this study, we report the presence and sequence characterization of an abundant reservoir of eccDNAs in both GS and GR biotypes using single molecule sequencing and the CIDER-Seq approach [18]. We examine the similarities and differences among samples representing distant geographic locations reported in [41], quantitate their abundance and diversity and assess whether recombination may be possible to form larger multimeric units.

Results

EccDNA content and coding structure in geographically distributed *A. palmeri*

147 Following the general methods and recommended computational pipelines
148 outlined in the CIDER-Seq single-molecule approach [42], we identified an extensive
149 amount of variable-sized eccDNA in all samples of (GS) and GR) biotypes that were
150 sequenced [Table 1]. The number of unique eccDNAs detected in GS samples ranged
151 from 443 (ks_s) to 6,227 (ms_s) with a mean of 2,661 [Table 1]. Unique eccDNAs were
152 in much higher abundance in GR samples and ranged from 2,200 (az_r) to 5,650
153 (ms_r), with a mean of 4,448, nearly double that of GS [Table 1]. Length distributions of
154 eccDNA were similar among both GS and GR biotypes and ranged from 27bp to nearly
155 27kb, with mean lengths of around 6kb, [Table 1 and Fig 1]. Gene prediction resulted in
156 eccDNAs both with and without complete open reading frames. In GS samples, the
157 number of eccDNAs with predicted genes ranged from 76-505 with a mean of 272
158 eccDNAs with genes per sample. GR eccDNAs with predicted genes was nearly 4
159 times greater with a range of 263-1,179 and a mean of 718 eccDNA with genes per
160 sample, suggesting that glyphosate stress influenced unique gene focal amplifications
161 [Table 1]. Of the eccDNA with predicted genes, the number of predicted genes per
162 eccDNA ranged from 1 to 10, with an average of 2 genes per eccDNA in both GS and
163 GR [S1 and S2 Tables]. Transfer RNAs (tRNA) were predicted exclusively on eccDNA
164 without CDS sequences and ranged widely from 46-715 (average of 350 per sample) in
165 GS and samples and 130-528 (average of 364 per sample).

166

167

168

Table 1. EccDNA characterization of GS and GR biotypes.

Sample biotype	# eccDNA	# eccDNA with Genes	# eccDNA with tRNA	% eccDNA with CDS	Length Distribution	Mean length
ks_s	443	76	46	17	60-22,237	5,906
ga_s	1564	257	183	16	57-22,477	6,273
az_r	2200	263	130	12	42-16,029	4461
az_s	2410	251	148	10	66-19,859	3999
ks_r	3234	578	267	18	35-23,960	6,400
de_r	4653	967	467	21	28-26,413	6668
ga_r	5138	978	528	19	30-23,670	6618
ms_r	5650	347	458	6	27-23,400	7,088
md_r	5817	1179	553	20	30-27,000	6,872
ms_s	6227	505	715	8	30-24,870	6,744

169

Fig 1. Frequency polygon graph for Lengths (bp) of *A. palmeri* eccDNAs. A) Glyphosate sensitive samples were sourced from Arizona (az_s), Georgia (ga_s), Kansas (ks_s), and Mississippi (ms_s) A. palmeri plants. B) Glyphosate resistant samples were sourced from Arizona (az_r), Delaware (de_r), Georgia (ga_r), Kansas (ks_r), Maryland (md_r), and Mississippi (ms_r) plants.

Coding content of eccDNAs in glyphosate sensitive and resistant *A. palmeri*

Gene content from both GS and GR biotypes was compared to identify unique and common functional protein coding domains among the geographically distant samples. In GS biotypes, 9 functional protein coding domains were discovered that are common among the each of the states [Fig 2]. These functional domains are annotated as ATP synthase, cytochrome P450, protein kinase, ribosomal protein, NADH dehydrogenase, Clp protease, and oxidoreductase [Table 2]. Various pairwise combinations of GS *A. palmeri* biotypes shared a range of 1 to 12 elements [Fig 2 and S3 Table]. Genes that regulate cell division, such as the Ras protein family and those involved in DNA replication (helicase) were common among Arizona, Georgia, and Mississippi GS eccDNA samples [S3 Table].

Fig 2. Venn diagram of PFAM elements shared by GS eccDNA samples. Arizona (az_s), Georgia (ga_s), Kansas (ks_s), and Mississippi (ms_s) sensitive A. palmeri eccDNA shared 9 total

Table 2. Gene elements shared by all sensitive eccDNA samples.

Total	PFAM Accession	Annotation
9	PF00006	ATP synthase alpha/beta family, nucleotide-binding domain
	PF00067	Cytochrome P450
	PF00069	Protein kinase domain

	PF00164	Ribosomal protein S12/S23
	PF00181	Ribosomal Proteins L2, RNA binding domain
	PF00346	Respiratory-chain NADH dehydrogenase, 49 Kd subunit
	PF00411	Ribosomal protein S11
	PF00574	Clp protease
	PF01058	NADH ubiquinone oxidoreductase, 20 Kd subunit

Several abiotic/biotic resilience-related functional protein domains were found in Arizona and Mississippi GS samples that includes an oxysterol-binding protein, pectinesterase, NmrA-like family, and WRKY DNA-binding domain elements [S3 Table]. Also discovered were shared functional domains involved in DNA methylation and histone maintenance (H2A/H2B/H3/H4) [S3 Table]. Common between Georgia and Mississippi GS biotypes were ABC transporter and Cytochrome C oxidase subunit II (periplasmic domain) protein domains [S3 Table]. Unique to Arizona were response regulators such as trehalose-phosphatase, chalcone-flavanone isomerase, O-methyltransferase, Myb-like DNA-binding domain [S3 Table]. Hundreds of other unique functional domains in different GS biotypes were recorded in S3 Table. It is notable that the *EPSPS* gene was not found in any of the GS eccDNAs.

In GR biotypes, we identified a total of 20 functional protein domains that are shared among all 6 resistant samples [Fig 3 and Table 3]. The shared GR domains had

Fig 3. Venn diagram of PFAM elements shared among GR *A. palmeri* eccDNA samples. Arizona (az_r), Delaware (de_r), Georgia (ga_r), Kansas (ks_r), Maryland (md_r), and Mississippi (ms_r) resistant A. palmeri eccDNA shared 20 total PFAM elements.

198 various cellular maintenance functions in addition to stress response domains that
199 include ABC transporter, HSP70 protein, Ribosomal protein, WD domain, and Leucine
200 rich repeats [Table 3]. A range of 1 to 9 protein family domains were shared by at least
201 5 of the GR biotypes [Fig 3 and S4 Table]. No apical meristem (NAM) protein,
202 peroxidase, TCP-1/cpn60 chaperonin family are among the stress response elements.
203 Arizona, Delaware, Kansas, and Maryland GR biotypes all contained EPSP synthase
204 (3-phosphoshikimate 1-carboxyvinyltransferase) and Arabidopsis phospholipase-like
205 protein (PEARLI 4) functional domains, with 21 and 24 copies distributed across various
206 eccDNA within these four samples respectively.

207

Table 3. Gene elements shared by all GR eccDNA samples.

Total	PFAM Accession	Annotation
20	PF00004	ATPase family associated with various cellular activities (AAA)
	PF00005	ABC transporter
	PF00006	ATP synthase alpha/beta family, nucleotide-binding domain
	PF00012	HSP70 protein
	PF00067	Cytochrome P450
	PF00069	Protein kinase domain
	PF00076	RNA recognition motif. (a.k.a. RRM, RBD, or RNP domain)
	PF00164	Ribosomal protein S12/S23
	PF00181	Ribosomal Proteins L2, RNA binding domain

	PF00306	ATP synthase alpha/beta chain, C terminal domain
	PF00346	Respiratory-chain NADH dehydrogenase, 49 Kd subunit
	PF00400	WD domain, G-beta repeat
	PF00411	Ribosomal protein S11
	PF00481	Protein phosphatase 2C
	PF00574	Clp protease
	PF01058	NADH ubiquinone oxidoreductase, 20 Kd subunit
	PF02874	ATP synthase alpha/beta family, beta-barrel domain
	PF03947	Ribosomal Proteins L2, C-terminal domain
	PF07714	Protein tyrosine and serine/threonine kinase
	PF13855	Leucine rich repeat

Gene ontology enrichment of *A. palmeri* eccDNA

Gene ontology enrichment analysis of predicted coding elements on eccDNA of GS eccDNA revealed a variety of enriched biological processes, cellular components, and molecular functions encoded on eccDNA [Fig 4]. Enriched biological processes include regulation of transcription, membrane and lipid transport, DNA binding, fatty acid biosynthesis, protein phosphorylation, oxidation-reduction, chromatin maintenance, and protein translation [Fig 4a and S5 Table]. Cellular component and molecular function

Fig 4. Gene ontology enrichment terms and their prevalence among GS *A. palmeri* eccDNA samples. **A.** Biological processes, **B.** cellular components, **C.** molecular functions.

categories of interest include membrane and ribosome components [Fig 4b], cytoplasm, protein kinase activity, and ATP binding [Fig 4c].

Glyphosate resistant eccDNAs showed similar, but slightly different enriched biological processes such as transmembrane transport, translation, protein phosphorylation, and oxidation-reduction process [Fig 5a]. Ribosome, nucleus, membrane, and integral component of membrane were also enriched in the cellular component category [Fig 5b]. Representative molecular functions for GR eccDNA were mainly in the ribosome and membrane categories, but ATP binding, protein kinase activity, and catalytic activity were enriched [Fig 5c and S6 Table].

Fig 5. Gene ontology enrichment terms and their prevalence among GR *A. palmeri* eccDNA samples**. A**. Biological processes, **B**. cellular components, **C**. molecular functions.

Repeat structure of *A. palmeri* eccDNA

Repeat characterization revealed a high proportion of repetitive sequences among both GS and GR eccDNAs [S7 Table]. The most common repeat classes were simple repeats, long terminal repeats (LTR) from the Copia superfamily, low complexity regions, and LTR from the Gypsy superfamily [S7 Table]. Interestingly, simple repeat content varied drastically among the GR and GS states. For example, Arizona and Mississippi GS and GR pairs were closely balanced in terms of content, but Mississippi has nearly 6 times as many with ~17.5k compared to ~4k simple repeats [S7 Table]. The Long Terminal Repeats/Copia class was second in abundance among eccDNAs, followed by low complexity repeats and then Gypsy elements. DNA elements such as

Stowaway, LINES, Cassandra, hAT-Tip100, MULE-MuDR, and helitrons were also identified in both GS and GR biotypes [S7 Table].

Similarity to the eccDNA replicon and replication origins on eccDNAs in *A. palmeri*

Alignment and comparative analysis for coding content and conserved sequence structure between GS and GR eccDNAs and the eccDNA replicon [26] identified a total of 162 GS eccDNA and 2,547 GR eccDNA with at matches at least 100 bp in length

244 with a percent identify of at least 95% [Fig 6]. A total of 7 and 11 eccDNA replicon
245 genes were predicted in GS and GR eccDNA, respectively [S8 Table]. Predicted

Fig 7. *EPSPS* gene copies in GR eccDNA. A. Sequence similarity of GR eccDNA aligned to the eccDNA replicon. Blue and orange links indicate single or duplicated EPSPS genes. Grey links show broader sequence similarities. B. Self-alignment of the GR eccDNA containing multiple EPSPS copies. Blue dots indicate inverted repeat sequences and red dots indicate repetitive sequence in the forward direction.

Fig 6. Alignment of eccDNA to the replicon in GS and GR biotypes. A. Alignment of 162 GS eccDNA to the eccDNA replicon. B. Alignment of 2,547 GR eccDNA to the eccDNA replicon. Red colors indicate indirect orientation and blue are direct. Alignments are filtered for matches of at least

246 eccDNA replicon genes in GS eccDNA include PEARLI4, Heat shock (HSP70), no
247 apical meristem (NAM), replication factor-A, retrotransposon, zinc finger, and
248 suppressor of gene silencing [S8 Table]. GR predicted replicon genes include: *EPSPS,*
249 PEARLI4, Domain of unknown function (DUF), ethylene response factor, HSP70, NAM,
250 replication factor A, and retrotransposon [S8 Table]. Interestingly, several GR eccDNA
251 contained multiple copies of the *EPSPS* gene from Arizona, Delaware, Kansas, and
252 Maryland, while the *EPSPS* gene was not present on any eccDNA in GS [Fig 7A].

253

254 In GR eccDNA we identified 5 eccDNA with 2 copies of the *EPSPS* gene and 11
255 eccDNA with a single *EPSPS* copy [Fig 7A]. A self-alignment of the GR *EPSPS*
256 eccDNA shows many conserved direct and indirect repeats [Fig 7B] with very high
257 sequence identity (>95% with at least 100bp). Palindromic repeats that flank the
258 *EPSPS* gene, previously described as possible genome tethering sites [26], were also
259 evident among various eccDNA (Grey links in A and on the top right corner of B)

indicating the potential for recombination among these smaller eccDNA, relative to the replicon.

Previous work has implicated a 17bp extended autonomous consensus sequence (EACS) with a motif of WWWWTTTAYRTTTWGTT that contains a core 11bp autonomous consensus sequence (ACS) reported in yeast [43] as a sequence where replication machinery initiates autonomous replication in plants [33]; which was functionally verified in the eccDNA replicon [35] [Fig 8]. Analysis of the GS and GR eccDNA for autonomous consensus (ACS) sequences (ACS) [43] identified a total of

Fig 8. Extended autonomous consensus sequence sequence (EACS) presented in [34]. The core autonomous consensus sequence is highlighted with the TAYR motif highlighted as the origin of replication complex binding site (ORC) and the TTT motif highlighted as a helicase binding site. 'W' denotes A or T, 'Y' denotes C or T, 'R' denotes G or A.

430 unique eccDNA with 16 of the 17 bp present in the EACS with the common missing base being the first 'W' (A or T), several of which had multiple EACS sequences [Fig 8 and S9 Table]. A total of 36,237 core ACS sites (11bp) were predicted within 18,679 unique eccDNA out of the total 37,336 predicted eccDNAs implicating this sequence as a possible common origin of replication sequence among smaller eccDNA in *Amaranthus palmeri.* Of the eccDNA that contained ARS sequences, 2,785 were predicted to contain coding sequences, whereas 16,048 eccDNA did not contain an ARS sequence.

Genomic origins of eccDNAs in *A. palmeri*

To determine the genomic origins of eccDNA and the possibility of genomic regions with a disposition for eccDNA formation, GS and GR eccDNA were mapped to

279 the chromosome scaffolded *Amaranthus palmeri* assembly [44] and counted using non-
280 overlapping genomic windows of 500kb [Fig 9]. We identified several regions of the
281 genome with a very high disposition for focal amplifications that are conserved between
282 GS and GR. These regions include the distal end of chromosome 2 and near the center
283 of chromosome 3, and several other regions distributed throughout the genome [Fig 9a].
284 The 500kb window localized at the distal end of chromosome 2 contained 285 eccDNA
285 from GS and 469 from GR [Fig 9a and S10 Table]. The center of chromosome 3

Fig 9. A. Alignment and quantification of unique eccDNA of GS (red) and GR (blue) to the chromosome-scale Palmer amaranthus reference assembly in 500kb non-overlapping windows. Darker colors represent a larger abundance of mapped eccDNA. Regions with the dotted ellipses indicate a high abundance of mapped eccDNA. **B.** Self-alignment of the 6 highlighted regions from A. Red dots indicated direct repeats, while blue are indirect. Regions highlighted in yellow are derived from the 2 genomic regions (2 & 3 - 500kb each) with the highest abundance of mapped eccDNA.

286 contained 225 GS and 449 GR eccDNA. The genomic region of eccDNA origin among
287 GR samples with the most eccDNA was on chromosome 4 with 487 eccDNA and only
288 51 from GS, suggesting a possible signal of glyphosate stress. Extraction and self-
289 alignment of the 6 genomic windows from the Palmer amaranth chromosome scale
290 assembly from [44] revealed intricate arrays of repetitive sequence [Fig 9b]. Short,
291 inverted repeats were the most common among all 6 regions [Fig 9b]. Clustered
292 palindromes of various sizes were discovered in segments 2, 3, 4, and 5, as indicated
293 by box-like structures. Regions 2 and 3 (highlighted in Fig 9b) contained more complex
294 repetitive structure with larger direct repeats (region 2) and indirect repeats (region 3)
295 [Fig 9b].

Discussion

Gene copy number variation is a predominant mechanism by which organisms respond to selective pressures in nature. Focal amplifications of transcriptionally active chromatin as eccDNAs have been found in both abundance and diversity across higher and lower order eukaryotic species underpinning their importance as a vehicle for gene copy amplification. Advancements of single molecule sequencing and approaches to purify and directly sequence circular DNA have led to evidence that eccDNA may have a fundamental role in the cell and function and also function as a source of genetic heterogeneity in response to environmental pressures [1-4, 22, 26, 31, 42]. Previous work in *Palmer amaranth* demonstrated that several genes in addition to *EPSPS* were co-amplified on a large eccDNA (~400kb) with sophisticated repetitive content and origins from distal segmental genomic regions [26]. This large eccDNA served as the vehicle for *EPSPS* gene copy amplification, but whether construction of this large eccDNA was the result of intramolecular recombination or recombination among a population of smaller eccDNA is unclear.

Using single molecule sequencing and the CIDER-Seq analytical pipeline [42], we identified diverse and abundant eccDNA species in both GS and GR biotypes collected from distal geographic regions that were previously reported [41]. The sizes of these eccDNA ranged from a few hundred base pairs to nearly 30kb in both biotypes and between 6 and 20% were predicted to contain genes which indicates that eccDNAs are present in *Amaranthus palmeri* without glyphosate exposure.

Gene enrichment analysis of both GS and GR eccDNA provided insight on biological processes and molecular functions enriched for activities related to a generalized stress response or important for rapid adaptation such as transcription regulation, development, chromatin, protein phosphorylation, oxidation-reduction, ribosomal and membrane components, protein kinase activity, and ATP binding. This indicates that eccDNAs may have a role in preserving important protein synthesis genes. Notably, transfer RNAs (tRNA) were predicted to reside on eccDNA in bothy GS and GR samples, but only on eccDNA that do not contain coding sequences. This was also shown by Wang et al., 2021 in Arabidopsis [19] and suggests that protein synthesis is a key attribute or component of the early response to stress and or the adaptive response. This finding also suggests that regulation of protein synthesis is perhaps as driven by eccDNA is an independent component of selection and directed gene focal amplifications as eccDNA. Furthermore, plants likely require additional copies of these protein synthesis genes for stress responses to produce significant immunity or defense products, as is the case for GR *A. palmeri* [1]. For example, transmembrane transport has been shown to plays an important role in adaptation of *Arabidopsis* to metalliferous soils [45], resource allocation and sensing under plant abiotic stress [46-48] and were enriched on GS *Palmer amaranth* eccDNA. Fatty acid biosynthesis is another category of enriched genes on GS eccDNA which has been implicated in signaling and plant defense to pathogens [49, 50].

At the gene level, there were a core set of 9 functional protein coding domains in common among the GS samples. Ribosomal proteins (circular rDNA), which are commonly reported as functional genes among eccDNA, were found among all 9 GS

341 samples suggesting a common role for rDNAs as circular structures in plants [6, 31, 51,
342 52]. Interestingly, Cytochrome p450 and Clp protease domains were also present in
343 each of the GS samples. Cytochrome p450s are a superfamily of genes that perform a
344 suite of functions in plant development and protection from various stresses via multiple
345 biosynthetic and detoxification pathways. Cytochrome p450 activity plays a central role
346 detoxification of xenobiotics in various weed species [53-56], biosynthesis of hormones,
347 fatty acids, sterols, cell wall components, biopolymers, and various defense compounds
348 [57]. Clp proteases are proteolytic enzymes whose increased expression also play a
349 protective role for the plant in both abiotic and biotic stress [58-60]. Clp proteases help
350 maintain protein homeostasis in chloroplasts and remove nonfunctional proteins, which
351 is essential during stress episodes when proteins tend to be more vulnerable to damage
352 [20–22]. These core genes encoded on GS eccDNA may contribute Palmer amaranth's
353 innate ability to rapidly adapt.

354 GS biotypes shared the same 9 core functional domains as GS biotypes
355 including Cytochrome p450 and Clp protease, in addition to 11 other domains indicating
356 that eccDNAs are dynamic and their presence and coding structure may be the result of
357 selective pressures. Notably, the additional functional domains in GR biotypes include
358 additional ribosomal motifs, ABC transporters, HSP70 proteins, and leucine rich repeat
359 (LRR) domains. ABC transporters are important for detoxification, environmental
360 stresses and pathogen resistance [23] and may play a complementary role in
361 glyphosate detoxification in addition to *EPSP* synthase over accumulation. The most
362 abundant functional domain and conserved among all the samples is the HSP70
363 domain; which functions in protein maintenance and a wide variety of stress response

364 mechanisms such as response to high temperatures [61], and was also a predicted
365 gene on the eccDNA replicon [26]. Hsp70 have been reported to function by holding
366 together protein substrates to help in movement, regulation, and prevent aggregation
367 under physical and or chemical pressure in plants [61, 62] and have served as
368 functional target in improving abiotic stress resilience in *Arabidopsis* [63] and other
369 species. It is notable that the HSP70 is present in both GS and GR biotypes but is a
370 core gene shared among all GR biotypes. The presence of Hsp70 on eccDNA
371 suggests a possible role in glyphosate resistance, or perhaps, a genomic mechanism
372 for rapid mitigation of heat and other abiotic stresses. Leucine rich repeat (LRR)
373 domains are associated with protein-protein interactions, often as part of plant innate
374 immune receptors [64]. Various transcription factors such as WRKY, bZIP, helicases,
375 GATA (zinc finger), E2F, helix-loop-helix, TCP, and others were also predicted on *A.*
376 *palmeri* eccDNA. Since transcription factor access to heterochromatin is limited by its
377 compact structure, eccDNAs may provide a faster and more effective avenue for protein
378 synthesis. Cancer cells with oncogenes encoded on eccDNAs appear to produce
379 significantly more transcript copies compared to the same oncogenes encoded on linear
380 DNA structures [14].

381 A primary question underlying the origins and structural dynamics of the large
382 eccDNA replicon (~400kb) [25, 26] is the mechanism by which it is assembled. The
383 most likely scenarios are long-range genomic interactions and a compounded building
384 event over short evolutionary time; or intramolecular recombination between smaller
385 eccDNA with newly selected genomic focal amplifications resulting from glyphosate
386 stress to form the larger structure, again over short evolutionary time scales. Here we

387 show a moderate degree of eccDNA replicon coverage with GS eccDNA [Fig 6a],
388 however there are large, disconnected gaps in coverage. It is notable that the *EPSPS*
389 gene was not found on any GS biotype eccDNA in this study, while several other
390 replicon genes were. One of the primary drawbacks to the CIDER-Seq methodology is
391 the limitation of eccDNA size to the read length of the Pacific Biosciences Sequel II
392 instrument [42] which means eccDNAs larger than an average read length will not be
393 sequenced intact, such as the eccDNA replicon [26]. This limitation prevented the
394 complete assembly of the *EPSPS* replicon, however the *EPSPS* gene and most other
395 predicted eccDNA replicon genes were found in GR biotype eccDNA and coverage of
396 the replicon was practically complete, with only a few small gaps. Furthermore, the
397 *EPSPS* gene was found on smaller eccDNA in GR biotypes in multiple copies, which
398 corroborates the work of Koo et al., that observed the extra-chromosomal *EPSPS* gene
399 vehicle as multi-meric forms. [25]. Together, these results suggest that eccDNA are
400 present as a basal source of genetic heterogeneity or rapid response mechanism, are
401 selectively amplified, and the large eccDNA structure reported to confer glyphosate
402 resistance is likely built by recombination among smaller eccDNA over rapid
403 evolutionary timescales.

404 Another important observation and similarity with the eccDNA replicon are the
405 high abundance and seemingly random distribution of the core 11bp autonomous
406 consensus sequence and a longer more conserved 16bp extended autonomous
407 consensus sequence [43] among approximately half of the GS and GR eccDNA. The
408 greater abundance seems to be on eccDNA without coding sequences. These
409 sequences were previously verified to function in autonomous replication and may be

410 regulated mechanism, perhaps epigenetic or other, to maintain gene copy numbers in
411 *A. palmeri*. In the eccDNA replicon, there is a single copy of the 17bp consensus
412 sequence and 46 copies of the 11bp sequence, seemingly randomly distributed among
413 the replicon [26, 35]. This observation further supports the possibility that the eccDNA
414 replicon is the result of recombination among smaller eccDNA. It is also possible that
415 there are alternate mechanisms or origins of replication on eccDNA in *A. palmeri* that
416 are used to maintain and amplify copy number. Previous work showed that the coding
417 components of the eccDNA replicon seem to be derived from distal regions of the
418 genome [26], and evidence presented here show that eccDNA in both GS and GR
419 seem to originate from all over the genome, Fig 9a. Here, we also demonstrate that
420 there are segments of the genome, or perhaps a genomic context, with a disposition for
421 focal amplifications. These genomic 'hotspots' are comprised of various repeat
422 structures that may have facilitate eccDNA formation. There are also regions of the
423 genome that seem to be activated as 'hotspots' in response to glyphosate stress that
424 suggests eccDNA formation may also be a directed event, rather than random. It is still
425 unclear if genes need to be in the 'right' genomic context for a focal amplification to
426 occur, or if other regulatory/initiation mechanisms exist. This work provides evidence
427 that eccDNA are a basal component of the cell and likely function as a reservoir of
428 genetic heterogeneity in *A. palmeri* as part of the rapid adaptation program.

429

430 Materials and methods

431 Plant material and genomic DNA extraction

Seeds were collected from individual GR plants that had survived glyphosate application as previously described [30, 41]. Plants were grown in 9 × 9 × 9 cm plastic pots that contained a commercial potting mix (Metro-Mix 360; Sun Gro Horticulture, Bellevue, WA, USA). Seeds were sown on the potting mix surface and lightly covered with 2 mm of potting mix. Pots were sub-irrigated and maintained in a greenhouse set at a temperature regime of 30/25 ∘C (day/night) and a 15-h photoperiod under natural sunlight conditions supplemented with high-pressure sodium lights providing 400 µmol m−2 s−1. Sampling for whole genome sequencing was performed using a leaf from the third node of two representative plants from each population. Total DNA was extracted using a modified CTAB-based protocol with chloroform, isopropanol, and RNase A buffer [65]. Briefly, leaf material from each sample (approximately 20-100 mg) was ground into a fine powder using a mortar and pestle with liquid nitrogen, extracted with CTAB buffer, chloroform extracted, and ethanol precipitated. Total genomic DNA was resuspended in 50 µl of TE (10 mM Tris, 0.1 m MEDTA, pH 8.0) buffer containing RNaseA. The tube was incubated at 37°C for 30 minutes and stored at -20°C.

EccDNA enrichment and sequencing (CIDER-seq)

Circular DNA enrichment sequencing (CIDER-Seq) was used to enrich, sequence, and analyze eccDNAs from the leaf tissue DNA extraction samples according to the protocol by Mehta et al., [17]. Because we wanted to survey the landscape of eccDNA, we did not perform a size exclusion step prior to enrichment. Otherwise, the circular DNA amplification, debranching reaction, and DNA branch release and repair stages closely

454 followed the methods of Mehta et al., [42]. Enriched eccDNA for each sample [10] was
455 individually barcoded following the manufacturer's recommended protocol (Pacific
456 Biosciences), pooled in equimolar amounts, and sequenced on a Sequel II single
457 molecule sequencer (Pacific Biosciences).

458 EccDNA sequence processing and analysis

459 Raw sequence reads were demultiplexed and circular consensus sequences
460 analyzed with the SMRT link software (Pacific Biosciences). Parameters for CCS
461 analysis were stringent and include: 1) predicted quality = 0.999; and 2) minimum read
462 length = 1,000 bp. Processed reads were stored as .fastq files. Processed fastq files
463 were analyzed with the packaged CIDER-seq software using the suggested approach to
464 identify circular DNA. Predicted eccDNA were matched to the *A. palmeri* reference
465 genome by Montgomery et al., [44]. After processing of predicted eccDNA, shorter
466 duplicate eccDNAs were collapsed into the longest reference eccDNA with the CDhit
467 software [66] with an identity threshold of 90%. Reference eccDNA were annotated for
468 genuine open reading frames using the MAKER annotation pipeline [67] and evidence
469 for genes derived from the *A. palmeri* published annotation [44]. Alignments to the
470 reference genome were performed with the Minimap2 software [68] and comparative
471 genome alignments performed with Mummer 4.0 [69]. Transfer RNAs were determined
472 with the tRNAscan-SE software with default settings [70]. The *A. palmeri* reference
473 assembly from [44] was divided into non-overlapping windows of 500kb and mapped
474 eccDNA counted with BedTools [71].

475 Acknowledgments

References

1. Gaubatz JW. Extrachromosomal circular DNAs and genomic sequence plasticity in eukaryotic cells. Mutat Res. 1990;237(5-6):271-92. Epub 1990/09/01. doi: 10.1016/0921-8734(90)90009-g. PubMed PMID: 2079966.

2. Cohen S, Regev A, Lavi S. Small polydispersed circular DNA (spcDNA) in human cells: association with genomic instability. Oncogene. 1997;14(8):977-85. Epub 1997/02/27. doi: 10.1038/sj.onc.1200917. PubMed PMID: 9050997.

3. Cohen S, Menut S, Mechali M. Regulated formation of extrachromosomal circular DNA molecules during development in Xenopus laevis. Mol Cell Biol. 1999;19(10):6682-9. Epub 1999/09/22. doi: 10.1128/MCB.19.10.6682. PubMed PMID: 10490607; PubMed Central PMCID: PMCPMC84653.

4. Cohen S, Yacobi K, Segal D. Extrachromosomal circular DNA of tandemly repeated genomic sequences in Drosophila. Genome Res. 2003;13(6A):1133-45. Epub 2003/06/12. doi: 10.1101/gr.907603. PubMed PMID: 12799349; PubMed Central PMCID: PMCPMC403641.

5. Moller HD, Parsons L, Jorgensen TS, Botstein D, Regenberg B. Extrachromosomal circular DNA is common in yeast. P Natl Acad Sci USA. 2015;112(24):E3114-E22. doi: 10.1073/pnas.1508825112. PubMed PMID: WOS:000356251800007.

6. Moller HD, Mohiyuddin M, Prada-Luengo I, Sailani MR, Halling JF, Plomgaard P, et al. Circular DNA elements of chromosomal origin are common in healthy human somatic tissue. Nat Commun. 2018;9(1):1069. Epub 2018/03/16. doi: 10.1038/s41467-018-03369-8. PubMed PMID: 29540679; PubMed Central PMCID: PMCPMC5852086.

499 7. Dillon LW, Kumar P, Shibata Y, Wang YH, Willcox S, Griffith JD, et al. Production
500 of Extrachromosomal MicroDNAs Is Linked to Mismatch Repair Pathways and
501 Transcriptional Activity. Cell Rep. 2015;11(11):1749-59. doi:
502 10.1016/j.celrep.2015.05.020. PubMed PMID: WOS:000356863600008.
503 8. Tomaska L, Nosek J, Kramara J, Griffith JD. Telomeric circles: universal players
504 in telomere maintenance? Nat Struct Mol Biol. 2009;16(10):1010-5. Epub 2009/10/08.
505 doi: 10.1038/nsmb.1660. PubMed PMID: 19809492; PubMed Central PMCID:
506 PMCPMC4041010.
507 9. Mazzucco G, Huda A, Galli M, Piccini D, Giannattasio M, Pessina F, et al.
508 Telomere damage induces internal loops that generate telomeric circles. Nature
509 Communications. 2020;11(1). doi: ARTN 5297

510 10.1038/s41467-020-19139-4. PubMed PMID: WOS:000585935900004.
511 10. Hull RM, Houseley J. The adaptive potential of circular DNA accumulation in
512 ageing cells. Curr Genet. 2020;66(5):889-94. Epub 2020/04/17. doi: 10.1007/s00294-
513 020-01069-9. PubMed PMID: 32296868; PubMed Central PMCID: PMCPMC7497353.
514 11. Yan Y, Guo G, Huang J, Gao M, Zhu Q, Zeng S, et al. Current understanding of
515 extrachromosomal circular DNA in cancer pathogenesis and therapeutic resistance. J
516 Hematol Oncol. 2020;13(1):124. Epub 2020/09/16. doi: 10.1186/s13045-020-00960-9.
517 PubMed PMID: 32928268; PubMed Central PMCID: PMCPMC7491193.
518 12. Wang T, Zhang H, Zhou Y, Shi J. Extrachromosomal circular DNA: a new
519 potential role in cancer progression. J Transl Med. 2021;19(1):257. Epub 2021/06/12.
520 doi: 10.1186/s12967-021-02927-x. PubMed PMID: 34112178; PubMed Central PMCID:
521 PMCPMC8194206.

522 13. Turner KM, Deshpande V, Beyter D, Koga T, Rusert J, Lee C, et al.
523 Extrachromosomal oncogene amplification drives tumour evolution and genetic
524 heterogeneity. Nature. 2017;543(7643):122-5. Epub 2017/02/09. doi:
525 10.1038/nature21356. PubMed PMID: 28178237; PubMed Central PMCID:
526 PMCPMC5334176.
527 14. Tandon I, Pal R, Pal JK, Sharma NK. Extrachromosomal circular DNAs: an extra
528 piece of evidence to depict tumor heterogeneity. Future Sci OA. 2019;5(6):FSO390.
529 Epub 2019/07/10. doi: 10.2144/fsoa-2019-0024. PubMed PMID: 31285839; PubMed
530 Central PMCID: PMCPMC6609892.
531 15. Wang M, Chen X, Yu F, Ding H, Zhang Y, Wang K. Extrachromosomal Circular
532 DNAs: Origin, formation and emerging function in Cancer. Int J Biol Sci.
533 2021;17(4):1010-25. Epub 2021/04/20. doi: 10.7150/ijbs.54614. PubMed PMID:
534 33867825; PubMed Central PMCID: PMCPMC8040306.
535 16. Wu SH, Turner KM, Nguyen N, Raviram R, Erb M, Santini J, et al. Circular
536 ecDNA promotes accessible chromatin and high oncogene expression. Nature.
537 2019;575(7784):699-+. doi: 10.1038/s41586-019-1763-5. PubMed PMID:
538 WOS:000500036800066.
539 17. Koche RP, Rodriguez-Fos E, Helmsauer K, Burkert M, MacArthur IC, Maag J, et
540 al. Extrachromosomal circular DNA drives oncogenic genome remodeling in
541 neuroblastoma. Nat Genet. 2020;52(1):29-34. Epub 2019/12/18. doi: 10.1038/s41588-
542 019-0547-z. PubMed PMID: 31844324; PubMed Central PMCID: PMCPMC7008131.
543 18. Mehta D, Cornet L, Hirsch-Hoffmann M, Zaidi SSEA, Vanderschuren H. Full-
544 length sequencing of circular DNA viruses and extrachromosomal circular DNA using

545 CIDER-Seq. Nat Protoc. 2020;15(5):1673-89. doi: 10.1038/s41596-020-0301-0.
546 PubMed PMID: WOS:000523115900001.
547 19. Wang K, Tian H, Wang L, Wang L, Tan Y, Zhang Z, et al. Deciphering
548 extrachromosomal circular DNA in Arabidopsis. Comput Struct Biotechnol J.
549 2021;19:1176-83. Epub 2021/03/09. doi: 10.1016/j.csbj.2021.01.043. PubMed PMID:
550 33680359; PubMed Central PMCID: PMCPMC7899950.
551 20. Navratilova A, Koblizkova A, Macas J. Survey of extrachromosomal circular DNA
552 derived from plant satellite repeats. BMC Plant Biol. 2008;8:90. Epub 2008/08/30. doi:
553 10.1186/1471-2229-8-90. PubMed PMID: 18721471; PubMed Central PMCID:
554 PMCPMC2543021.
555 21. Kinoshita Y, Ohnishi N, Yamada Y, Kunisada T, Yamagishi H. Extrachromosomal
556 Circular DNA from Nuclear Fraction of Higher-Plants. Plant Cell Physiol.
557 1985;26(7):1401-9. PubMed PMID: WOS:A1985ASZ0400021.
558 22. Cohen S, Houben A, Segal D. Extrachromosomal circular DNA derived from
559 tandemly repeated genomic sequences in plants. Plant J. 2008;53(6):1027-34. Epub
560 2007/12/20. doi: 10.1111/j.1365-313X.2007.03394.x. PubMed PMID: 18088310.
561 23. Thieme M, Lanciano S, Balzergue S, Daccord N, Mirouze M, Bucher E. Inhibition
562 of RNA polymerase II allows controlled mobilisation of retrotransposons for plant
563 breeding. Genome Biol. 2017;18(1):134. Epub 2017/07/09. doi: 10.1186/s13059-017-
564 1265-4. PubMed PMID: 28687080; PubMed Central PMCID: PMCPMC5501947.
565 24. Wu S, Turner KM, Nguyen N, Raviram R, Erb M, Santini J, et al. Circular ecDNA
566 promotes accessible chromatin and high oncogene expression. Nature.

2019;575(7784):699-703. Epub 2019/11/22. doi: 10.1038/s41586-019-1763-5. PubMed PMID: 31748743; PubMed Central PMCID: PMCPMC7094777.

25. Koo DH, Molin WT, Saski CA, Jiang J, Putta K, Jugulam M, et al. Extrachromosomal circular DNA-based amplification and transmission of herbicide resistance in crop weed Amaranthus palmeri. P Natl Acad Sci USA. 2018;115(13):3332-7. doi: 10.1073/pnas.1719354115. PubMed PMID: WOS:000428382400050.

26. Molin WT, Yaguchi A, Blenner M, Saski CA. The EccDNA Replicon: A Heritable, Extranuclear Vehicle That Enables Gene Amplification and Glyphosate Resistance in Amaranthus palmeri. Plant Cell. 2020;32(7):2132-40. doi: 10.1105/tpc.20.00099. PubMed PMID: WOS:000545974100017.

27. Gaines TA, Zhang W, Wang D, Bukun B, Chisholm ST, Shaner DL, et al. Gene amplification confers glyphosate resistance in Amaranthus palmeri. Proc Natl Acad Sci U S A. 2010;107(3):1029-34. Epub 2009/12/19. doi: 10.1073/pnas.0906649107. PubMed PMID: 20018685; PubMed Central PMCID: PMCPMC2824275.

28. Funke T, Han H, Healy-Fried ML, Fischer M, Schonbrunn E. Molecular basis for the herbicide resistance of Roundup Ready crops. Proc Natl Acad Sci U S A. 2006;103(35):13010-5. Epub 2006/08/19. doi: 10.1073/pnas.0603638103. PubMed PMID: 16916934; PubMed Central PMCID: PMCPMC1559744.

29. Sammons RD, Gaines TA. Glyphosate resistance: state of knowledge. Pest Manag Sci. 2014;70(9):1367-77. Epub 2014/09/03. doi: 10.1002/ps.3743. PubMed PMID: 25180399; PubMed Central PMCID: PMCPMC4260172.

30. Molin WT, Wright AA, Lawton-Rauh A, Saski CA. The unique genomic landscape surrounding the EPSPS gene in glyphosate resistant Amaranthus palmeri: a repetitive

590 path to resistance. BMC Genomics. 2017;18(1):91. Epub 2017/01/18. doi:
591 10.1186/s12864-016-3336-4. PubMed PMID: 28095770; PubMed Central PMCID:
592 PMCPMC5240378.
593 31. Cohen S, Agmon N, Sobol O, Segal D. Extrachromosomal circles of satellite
594 repeats and 5S ribosomal DNA in human cells. Mob DNA. 2010;1(1):11. Epub
595 2010/03/17. doi: 10.1186/1759-8753-1-11. PubMed PMID: 20226008; PubMed Central
596 PMCID: PMCPMC3225859.
597 32. Stinchcomb DT, Struhl K, Davis RW. Isolation and characterisation of a yeast
598 chromosomal replicator. Nature. 1979;282(5734):39-43. Epub 1979/11/01. doi:
599 10.1038/282039a0. PubMed PMID: 388229.
600 33. Eckdahl TT, Bennetzen JL, Anderson JN. DNA structures associated with
601 autonomously replicating sequences from plants. Plant Mol Biol. 1989;12(5):507-16.
602 Epub 1989/05/01. doi: 10.1007/BF00036965. PubMed PMID: 24271067.
603 34. Kowalski D, Eddy MJ. The DNA Unwinding Element - a Novel, Cis-Acting
604 Component That Facilitates Opening of the Escherichia-Coli Replication Origin. Embo J.
605 1989;8(13):4335-44. doi: DOI 10.1002/j.1460-2075.1989.tb08620.x. PubMed PMID:
606 WOS:A1989CE21700044.
607 35. Molin WT, Yaguchi A, Blenner M, Saski CA. Autonomous replication sequences
608 from the Amaranthus palmeri eccDNA replicon enable replication in yeast. BMC Res
609 Notes. 2020;13(1):330. Epub 2020/07/12. doi: 10.1186/s13104-020-05169-0. PubMed
610 PMID: 32650810; PubMed Central PMCID: PMCPMC7350638.
611 36. Feeney KM, Parish JL. Targeting mitotic chromosomes: a conserved mechanism
612 to ensure viral genome persistence. Proc Biol Sci. 2009;276(1662):1535-44. Epub

613 2009/02/11. doi: 10.1098/rspb.2008.1642. PubMed PMID: 19203914; PubMed Central
614 PMCID: PMCPMC2660980.
615 37. Gaines TA, Shaner DL, Ward SM, Leach JE, Preston C, Westra P. Mechanism of
616 resistance of evolved glyphosate-resistant Palmer amaranth (Amaranthus palmeri). J
617 Agric Food Chem. 2011;59(11):5886-9. Epub 2011/02/19. doi: 10.1021/jf104719k.
618 PubMed PMID: 21329355.
619 38. Kupper A, Borgato EA, Patterson EL, Netto AG, Nicolai M, de Carvalho SJP, et
620 al. Multiple Resistance to Glyphosate and Acetolactate Synthase Inhibitors in Palmer
621 Amaranth (Amaranthus palmeri) Identified in Brazil. Weed Sci. 2017;65(3):317-26. doi:
622 10.1017/wsc.2017.1. PubMed PMID: WOS:000405094400001.
623 39. Culpepper AS, Grey TL, Vencill WK, Kichler JM, Webster TM, Brown SM, et al.
624 Glyphosate-resistant Palmer amaranth (Amaranthus palmeri) confirmed in Georgia.
625 Weed Sci. 2006;54(4):620-6. doi: Doi 10.1614/Ws-06-001r.1. PubMed PMID:
626 WOS:000239469200003.
627 40. Molin WT, Wright AA, VanGessel MJ, McCloskey WB, Jugulam M, Hoagland RE.
628 Survey of the genomic landscape surrounding the 5-enolpyruvylshikimate-3-phosphate
629 synthase (EPSPS) gene in glyphosate-resistant Amaranthus palmeri from
630 geographically distant populations in the USA. Pest Manag Sci. 2018;74(5):1109-17.
631 Epub 2017/07/08. doi: 10.1002/ps.4659. PubMed PMID: 28686355.
632 41. Molin WT, Patterson EL, Saski CA. Homogeneity among glyphosate-resistant
633 Amaranthus palmeri in geographically distant locations. PLoS One.
634 2020;15(9):e0233813. Epub 2020/09/10. doi: 10.1371/journal.pone.0233813. PubMed
635 PMID: 32903277; PubMed Central PMCID: PMCPMC7480871.

636 42. Mehta D, Cornet L, Hirsch-Hoffmann M, Zaidi SS, Vanderschuren H. Full-length
637 sequencing of circular DNA viruses and extrachromosomal circular DNA using CIDER-
638 Seq. Nat Protoc. 2020;15(5):1673-89. Epub 2020/04/05. doi: 10.1038/s41596-020-
639 0301-0. PubMed PMID: 32246135.
640 43. Chang F, May CD, Hoggard T, Miller J, Fox CA, Weinreich M. High-resolution
641 analysis of four efficient yeast replication origins reveals new insights into the ORC and
642 putative MCM binding elements. Nucleic Acids Res. 2011;39(15):6523-35. Epub
643 2011/05/12. doi: 10.1093/nar/gkr301. PubMed PMID: 21558171; PubMed Central
644 PMCID: PMCPMC3159467.
645 44. Montgomery JS, Giacomini D, Waithaka B, Lanz C, Murphy BP, Campe R, et al.
646 Draft Genomes of Amaranthus tuberculatus, Amaranthus hybridus, and Amaranthus
647 palmeri. Genome Biol Evol. 2020;12(11):1988-93. Epub 2020/08/25. doi:
648 10.1093/gbe/evaa177. PubMed PMID: 32835372; PubMed Central PMCID:
649 PMCPMC7643611.
650 45. Sailer C, Babst-Kostecka A, Fischer MC, Zoller S, Widmer A, Vollenweider P, et
651 al. Transmembrane transport and stress response genes play an important role in
652 adaptation of Arabidopsis halleri to metalliferous soils. Sci Rep. 2018;8(1):16085. Epub
653 2018/11/02. doi: 10.1038/s41598-018-33938-2. PubMed PMID: 30382172; PubMed
654 Central PMCID: PMCPMC6208402.
655 46. Keller I, Rodrigues CM, Neuhaus HE, Pommerrenig B. Improved resource
656 allocation and stabilization of yield under abiotic stress. J Plant Physiol.
657 2021;257:153336. Epub 2020/12/29. doi: 10.1016/j.jplph.2020.153336. PubMed PMID:
658 33360492.

659 47. Shabala S, Bose J, Fuglsang AT, Pottosin I. On a quest for stress tolerance
660 genes: membrane transporters in sensing and adapting to hostile soils. J Exp Bot.
661 2016;67(4):1015-31. Epub 2015/10/29. doi: 10.1093/jxb/erv465. PubMed PMID:
662 26507891.
663 48. Zhu JK. Abiotic Stress Signaling and Responses in Plants. Cell.
664 2016;167(2):313-24. Epub 2016/10/08. doi: 10.1016/j.cell.2016.08.029. PubMed PMID:
665 27716505; PubMed Central PMCID: PMCPMC5104190.
666 49. Raffaele S, Leger A, Roby D. Very long chain fatty acid and lipid signaling in the
667 response of plants to pathogens. Plant Signal Behav. 2009;4(2):94-9. doi: DOI
668 10.4161/psb.4.2.7580. PubMed PMID: WOS:000213940700004.
669 50. Lim GH, Singhal R, Kachroo A, Kachroo P. Fatty Acid- and Lipid-Mediated
670 Signaling in Plant Defense. Annu Rev Phytopathol. 2017;55:505-36. Epub 2017/08/05.
671 doi: 10.1146/annurev-phyto-080516-035406. PubMed PMID: 28777926.
672 51. Cao X, Wang S, Ge L, Zhang W, Huang J, Sun W. Extrachromosomal Circular
673 DNA: Category, Biogenesis, Recognition, and Functions. Front Vet Sci. 2021;8:693641.
674 Epub 2021/09/28. doi: 10.3389/fvets.2021.693641. PubMed PMID: 34568472; PubMed
675 Central PMCID: PMCPMC8458813.
676 52. Sinclair DA, Guarente L. Extrachromosomal rDNA circles--a cause of aging in
677 yeast. Cell. 1997;91(7):1033-42. Epub 1998/01/15. doi: 10.1016/s0092-8674(00)80493-
678 6. PubMed PMID: 9428525.
679 53. Yanniccari M, Gigon R, Larsen A. Cytochrome P450 Herbicide Metabolism as
680 the Main Mechanism of Cross-Resistance to ACCase- and ALS-Inhibitors in Lolium spp.

681 Populations From Argentina: A Molecular Approach in Characterization and Detection.
682 Front Plant Sci. 2020;11. doi: ARTN 600301
683 10.3389/fpls.2020.600301. PubMed PMID: WOS:000593945200001.
684 54. Busi R, Vila-Aiub MM, Powles SB. Genetic control of a cytochrome P450
685 metabolism-based herbicide resistance mechanism in Lolium rigidum. Heredity (Edinb).
686 2011;106(5):817-24. Epub 2010/09/30. doi: 10.1038/hdy.2010.124. PubMed PMID:
687 20877397; PubMed Central PMCID: PMCPMC3186236.
688 55. Li Q, Fang Y, Li X, Zhang H, Liu M, Yang H, et al. Mechanism of the plant
689 cytochrome P450 for herbicide resistance: a modelling study. J Enzyme Inhib Med
690 Chem. 2013;28(6):1182-91. Epub 2012/10/13. doi: 10.3109/14756366.2012.719505.
691 PubMed PMID: 23057845.
692 56. Dimaano NG, Iwakami S. Cytochrome P450-mediated herbicide metabolism in
693 plants: current understanding and prospects. Pest Manag Sci. 2021;77(1):22-32. Epub
694 2020/08/11. doi: 10.1002/ps.6040. PubMed PMID: 32776423.
695 57. Pandian BA, Sathishraj R, Djanaguiraman M, Prasad PVV, Jugulam M. Role of
696 Cytochrome P450 Enzymes in Plant Stress Response. Antioxidants (Basel). 2020;9(5).
697 Epub 2020/05/30. doi: 10.3390/antiox9050454. PubMed PMID: 32466087; PubMed
698 Central PMCID: PMCPMC7278705.
699 58. Ali MS, Baek KH. Protective Roles of Cytosolic and Plastidal Proteasomes on
700 Abiotic Stress and Pathogen Invasion. Plants (Basel). 2020;9(7). Epub 2020/07/08. doi:
701 10.3390/plants9070832. PubMed PMID: 32630761; PubMed Central PMCID:
702 PMCPMC7412383.

703 59. Torres MA, Dangl JL. Functions of the respiratory burst oxidase in biotic
704 interactions, abiotic stress and development. Curr Opin Plant Biol. 2005;8(4):397-403.
705 Epub 2005/06/09. doi: 10.1016/j.pbi.2005.05.014. PubMed PMID: 15939662.
706 60. Baek KH, Choi D. Roles of Plant Proteases in Pathogen Defense. Plant
707 Pathology J. 2008;24(4):367-74. doi: Doi 10.5423/Ppj.2008.24.4.367. PubMed PMID:
708 WOS:000261334900001.
709 61. Usman MG, Rafii MY, Martini MY, Yusuff OA, Ismail MR, Miah G. Molecular
710 analysis of Hsp70 mechanisms in plants and their function in response to stress.
711 Biotechnol Genet Eng Rev. 2017;33(1):26-39. Epub 2017/06/27. doi:
712 10.1080/02648725.2017.1340546. PubMed PMID: 28649918.
713 62. Alderson TR, Kim JH, Markley JL. Dynamical Structures of Hsp70 and Hsp70-
714 Hsp40 Complexes. Structure. 2016;24(7):1014-30. Epub 2016/06/28. doi:
715 10.1016/j.str.2016.05.011. PubMed PMID: 27345933; PubMed Central PMCID:
716 PMCPMC4938735.
717 63. Masand S, Yadav SK. Overexpression of MuHSP70 gene from Macrotyloma
718 uniflorum confers multiple abiotic stress tolerance in transgenic Arabidopsis thaliana.
719 Mol Biol Rep. 2016;43(2):53-64. Epub 2015/12/24. doi: 10.1007/s11033-015-3938-y.
720 PubMed PMID: 26694324.
721 64. Padmanabhan M, Cournoyer P, Dinesh-Kumar SP. The leucine-rich repeat
722 domain in plant innate immunity: a wealth of possibilities. Cell Microbiol.
723 2009;11(2):191-8. Epub 2008/11/20. doi: 10.1111/j.1462-5822.2008.01260.x. PubMed
724 PMID: 19016785; PubMed Central PMCID: PMCPMC2762402.

65. Molin WT, Wright AA, VanGessel MJ, McCloskey WB, Jugulam M, Hoagland RE. Survey of the genomic landscape surrounding the 5-enolpyruvylshikimate-3-phosphate synthase (EPSPS) gene in glyphosate-resistant Amaranthus palmeri from geographically distant populations in the USA. Pest Management Science. 2018;74(5):1109-17. doi: 10.1002/ps.4659. PubMed PMID: WOS:000428524600013.

66. Li W, Godzik A. Cd-hit: a fast program for clustering and comparing large sets of protein or nucleotide sequences. Bioinformatics. 2006;22(13):1658-9. Epub 2006/05/30. doi: 10.1093/bioinformatics/btl158. PubMed PMID: 16731699.

67. Cantarel BL, Korf I, Robb SM, Parra G, Ross E, Moore B, et al. MAKER: an easy-to-use annotation pipeline designed for emerging model organism genomes. Genome Res. 2008;18(1):188-96. Epub 2007/11/21. doi: 10.1101/gr.6743907. PubMed PMID: 18025269; PubMed Central PMCID: PMCPMC2134774.

68. Li H. Minimap2: pairwise alignment for nucleotide sequences. Bioinformatics. 2018;34(18):3094-100. Epub 2018/05/12. doi: 10.1093/bioinformatics/bty191. PubMed PMID: 29750242; PubMed Central PMCID: PMCPMC6137996.

69. Marcais G, Delcher AL, Phillippy AM, Coston R, Salzberg SL, Zimin A. MUMmer4: A fast and versatile genome alignment system. PLoS Comput Biol. 2018;14(1):e1005944. Epub 2018/01/27. doi: 10.1371/journal.pcbi.1005944. PubMed PMID: 29373581; PubMed Central PMCID: PMCPMC5802927.

70. Chan PP, Lowe TM. tRNAscan-SE: Searching for tRNA Genes in Genomic Sequences. Methods Mol Biol. 2019;1962:1-14. Epub 2019/04/26. doi: 10.1007/978-1-4939-9173-0_1. PubMed PMID: 31020551; PubMed Central PMCID: PMCPMC6768409.

748 71. Quinlan AR. BEDTools: The Swiss-Army Tool for Genome Feature Analysis.
749 Curr Protoc Bioinformatics. 2014;47:11 2 1-34. Epub 2014/09/10. doi:
750 10.1002/0471250953.bi1112s47. PubMed PMID: 25199790; PubMed Central PMCID:
751 PMCPMC4213956.

752

753 Supporting information

754 **S1 Table.** Summary and functional annotation of glyphosate sensitive eccDNAs.

755 **S2 Table.** Summary and functional annotation of glyphosate resistant eccDNAs.

756 **S3 Table.** Venn diagram result summary for glyphosate sensitive eccDNA samples with
757 annotations.

758 **S4 Table.** Venn diagram result summary for glyphosate resistant eccDNA samples with
759 annotations.

760 **S5 Table.** Gene ontology enrichment of all glyphosate sensitive eccDNA genes
761 classified as biological **process (BP), cellular component (CC), and molecular**
762 **function (MF).**

763 **S6 Table.** Gene ontology enrichment of all glyphosate resistant eccDNA genes
764 classified as biological process (BP), cellular component (CC), and molecular function
765 (MF).

766 **S7 Table.** Repeat characterization of eccDNA in glyphosate sensitive and resistant
767 samples.

768 **S8 Table.** Summary and functional annotation of predicted eccDNAs in glyphosate

769 sensitive and resistant biotypes from different states.

770 **S9 Table.** eccDNA with predicted EACs or ACS sequence.

771 **S10 Table.** Counts of eccDNA mapping to the *A. palmeri* genome.

772

773

774

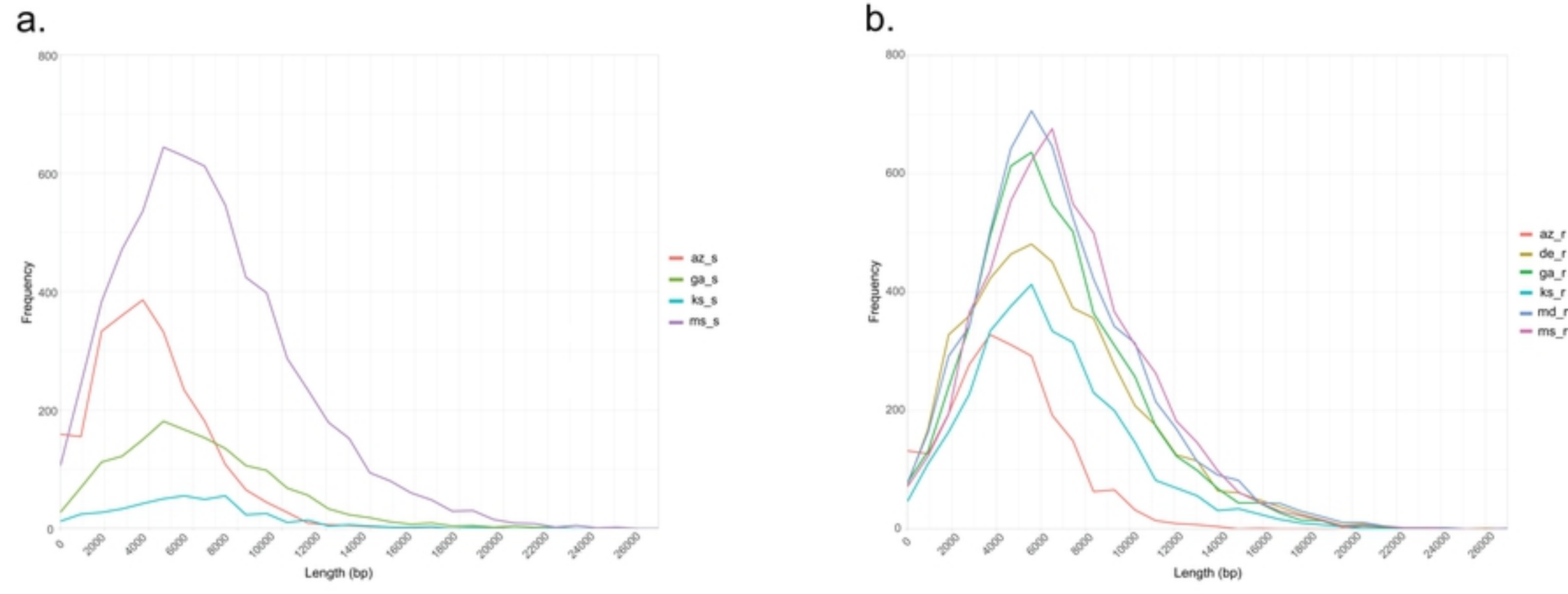

Fig 1

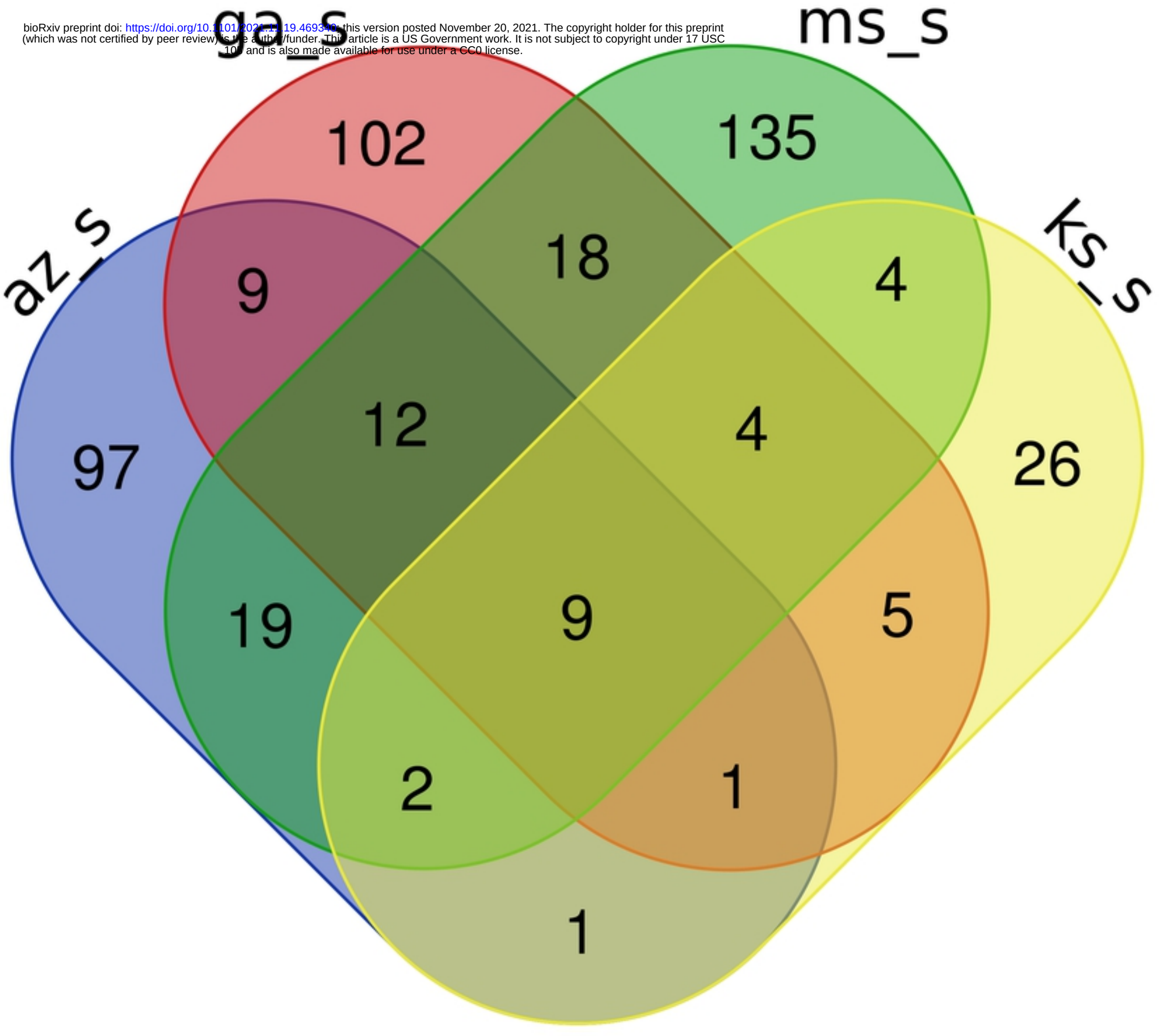

Fig 2

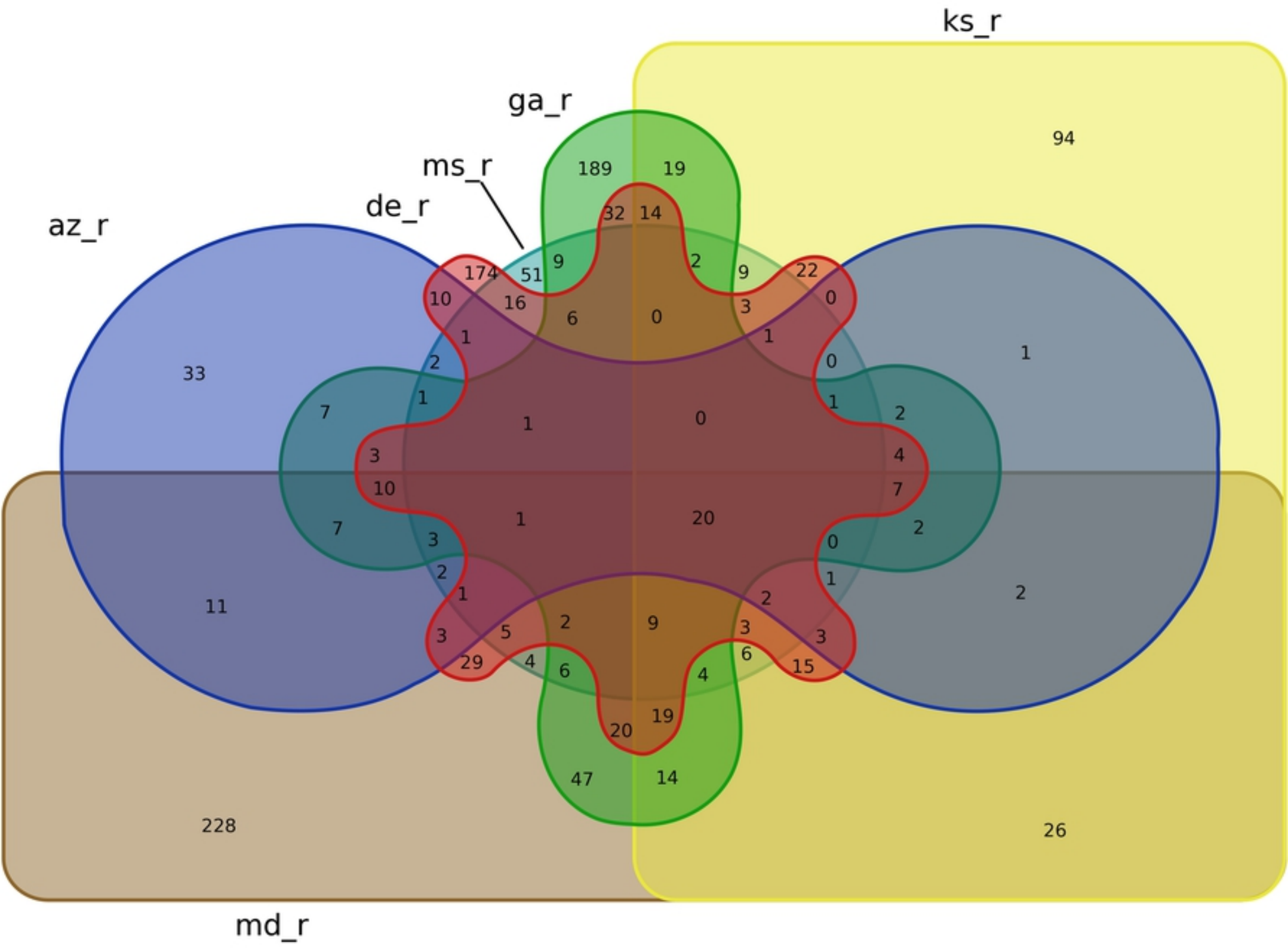
ks_r
ga_r
ms_r
de_r
az_r
md_r
94
189
19
32
14
174
51
9
2
9
22
10
16
6
0
3
0
1
1
33
2
0
1
1
7
1
0
2
3
4
10
7
1
20
7
2
3
0
2
1
11
1
2
2
9
3
3
5
3
29
4
6
6
4
15
19
20
47
14
228
26

Fig 3

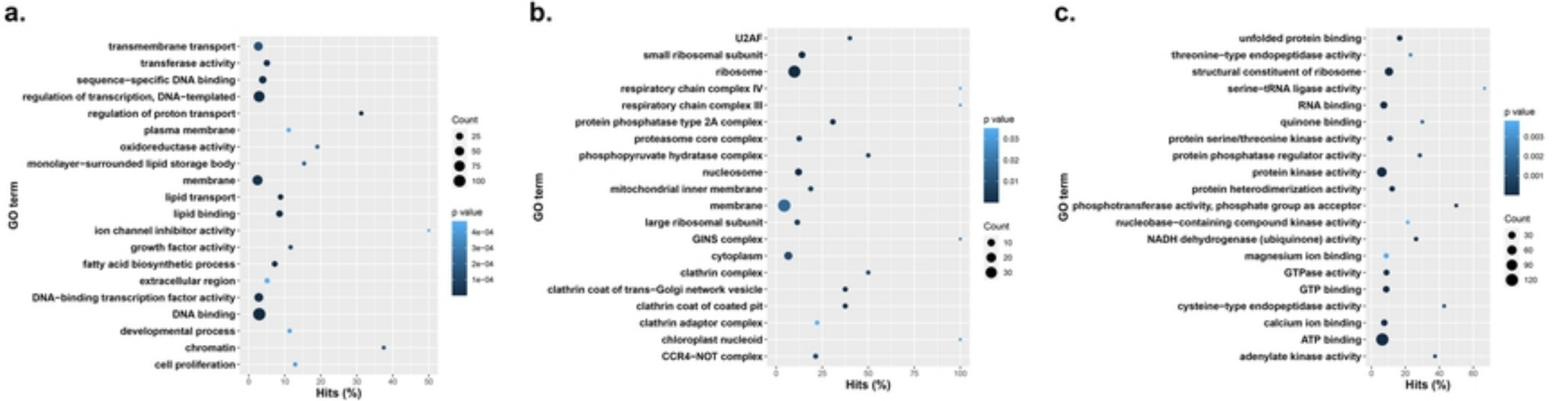
a.
transmembrane transport
transferase activity
sequence−specific DNA binding
regulation of transcription, DNA−templated
regulation of proton transport
plasma membrane
oxidoreductase activity
monolayer−surrounded lipid storage body
membrane
lipid transport
lipid binding
ion channel inhibitor activity
growth factor activity
fatty acid biosynthetic process
extracellular region
DNA−binding transcription factor activity
DNA binding
developmental process
chromatin
cell proliferation
GO term
Hits (%)
Count
p value
b.
U2AF
small ribosomal subunit
ribosome
respiratory chain complex IV
respiratory chain complex III
protein phosphatase type 2A complex
proteasome core complex
phosphopyruvate hydratase complex
nucleosome
mitochondrial inner membrane
membrane
large ribosomal subunit
GINS complex
cytoplasm
clathrin complex
clathrin coat of trans−Golgi network vesicle
clathrin coat of coated pit
clathrin adaptor complex
chloroplast nucleoid
CCR4−NOT complex
GO term
Hits (%)
p value
Count
c.
unfolded protein binding
threonine−type endopeptidase activity
structural constituent of ribosome
serine−tRNA ligase activity
RNA binding
quinone binding
protein serine/threonine kinase activity
protein phosphatase regulator activity
protein kinase activity
protein heterodimerization activity
phosphotransferase activity, phosphate group as acceptor
nucleobase−containing compound kinase activity
NADH dehydrogenase (ubiquinone) activity
magnesium ion binding
GTPase activity
GTP binding
cysteine−type endopeptidase activity
calcium ion binding
ATP binding
adenylate kinase activity
GO term
Hits (%)
p value
Count

Fig 4

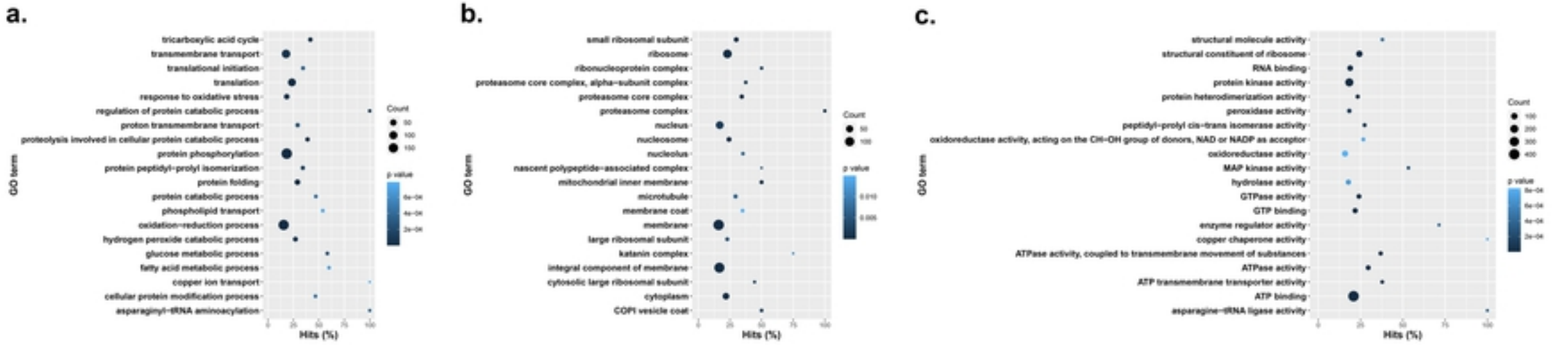
a.
tricarboxylic acid cycle
transmembrane transport
translational initiation
translation
response to oxidative stress
regulation of protein catabolic process
proton transmembrane transport
proteolysis involved in cellular protein catabolic process
protein phosphorylation
protein peptidyl-prolyl isomerization
protein folding
protein catabolic process
phospholipid transport
oxidation-reduction process
hydrogen peroxide catabolic process
glucose metabolic process
fatty acid metabolic process
copper ion transport
cellular protein modification process
asparaginyl-tRNA aminoacylation
GO term
Hits (%)
Count
p value
b.
small ribosomal subunit
ribosome
ribonucleoprotein complex
proteasome core complex, alpha-subunit complex
proteasome core complex
proteasome complex
nucleus
nucleosome
nucleolus
nascent polypeptide-associated complex
mitochondrial inner membrane
microtubule
membrane coat
membrane
large ribosomal subunit
katanin complex
integral component of membrane
cytosolic large ribosomal subunit
cytoplasm
COPI vesicle coat
GO term
Hits (%)
Count
p value
c.
structural molecule activity
structural constituent of ribosome
RNA binding
protein kinase activity
protein heterodimerization activity
peroxidase activity
peptidyl-prolyl cis-trans isomerase activity
oxidoreductase activity, acting on the CH-OH group of donors, NAD or NADP as acceptor
oxidoreductase activity
MAP kinase activity
hydrolase activity
GTPase activity
GTP binding
enzyme regulator activity
copper chaperone activity
ATPase activity, coupled to transmembrane movement of substances
ATPase activity
ATP transmembrane transporter activity
ATP binding
asparagine-tRNA ligase activity
GO term
Hits (%)
Count
p value

Fig 5

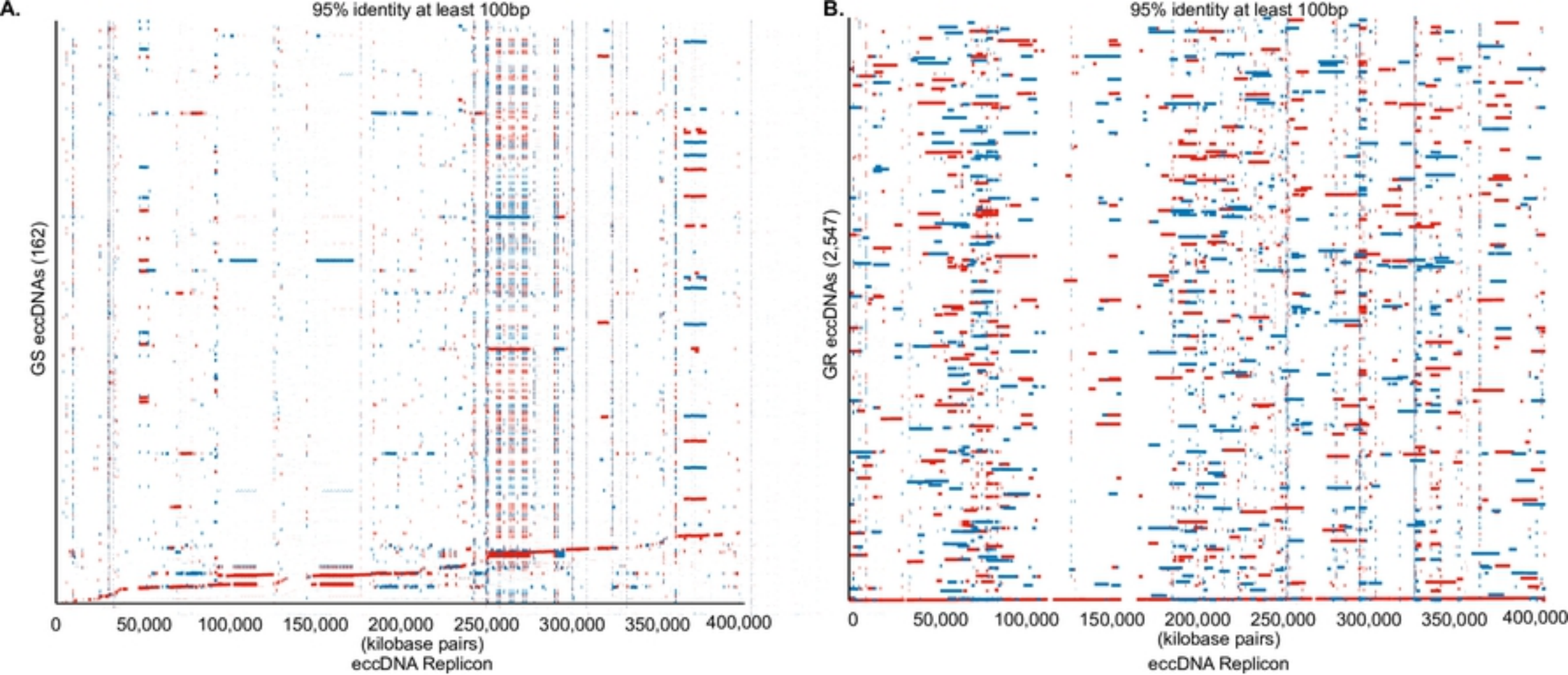
A.
95% identity at least 100bp
GS eccDNAs (162)
0
50,000
100,000
150,000
200,000
250,000
300,000
350,000
400,000
(kilobase pairs)
eccDNA Replicon
B.
95% identity at least 100bp
GR eccDNAs (2,547)
0
50,000
100,000
150,000
200,000
250,000
300,000
350,000
400,000
(kilobase pairs)
eccDNA Replicon

Fig 6

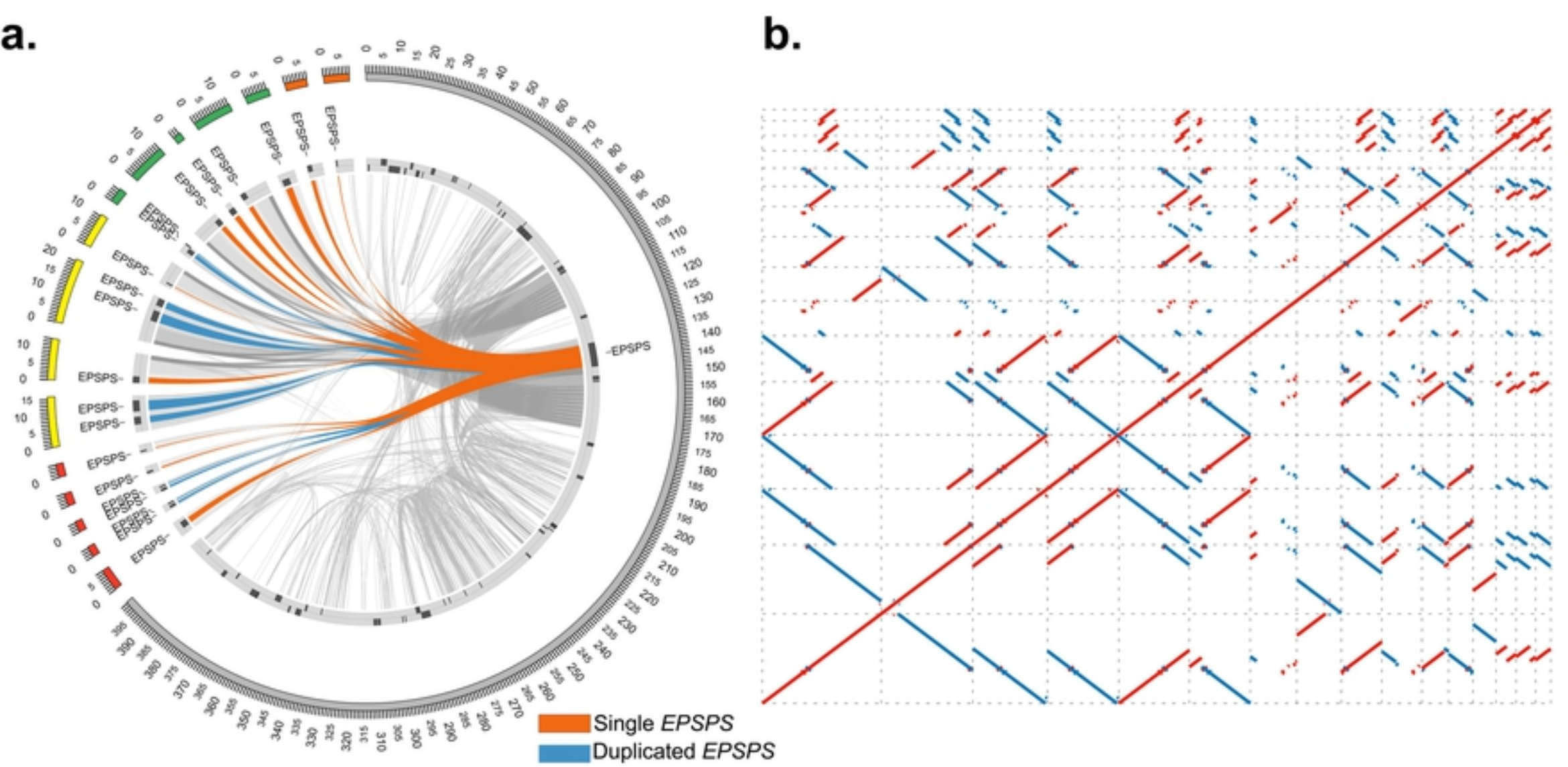

Fig 7

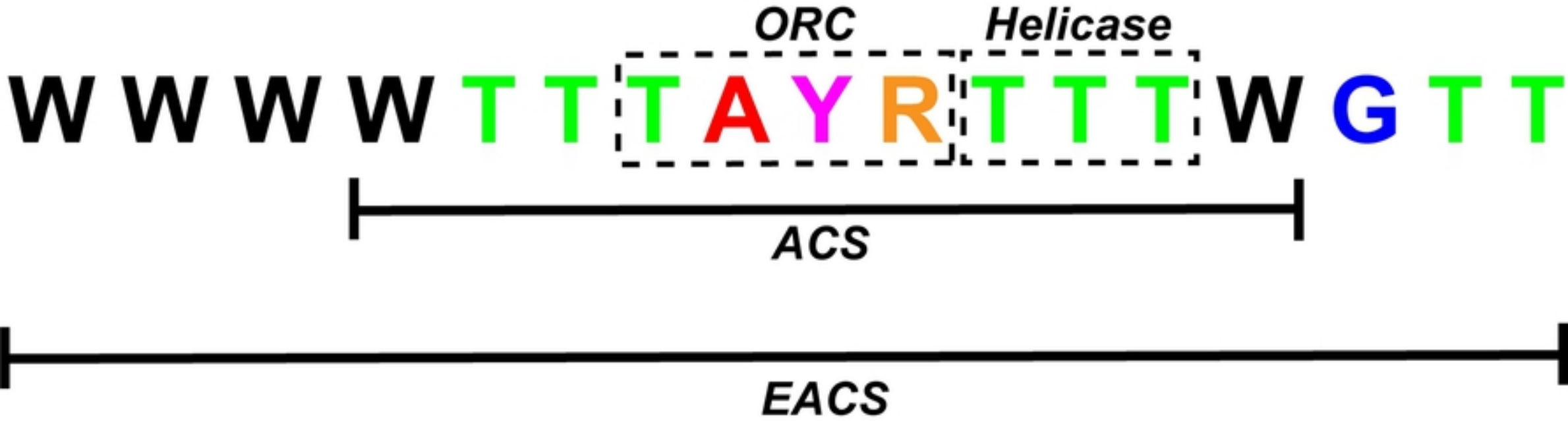

Fig 8

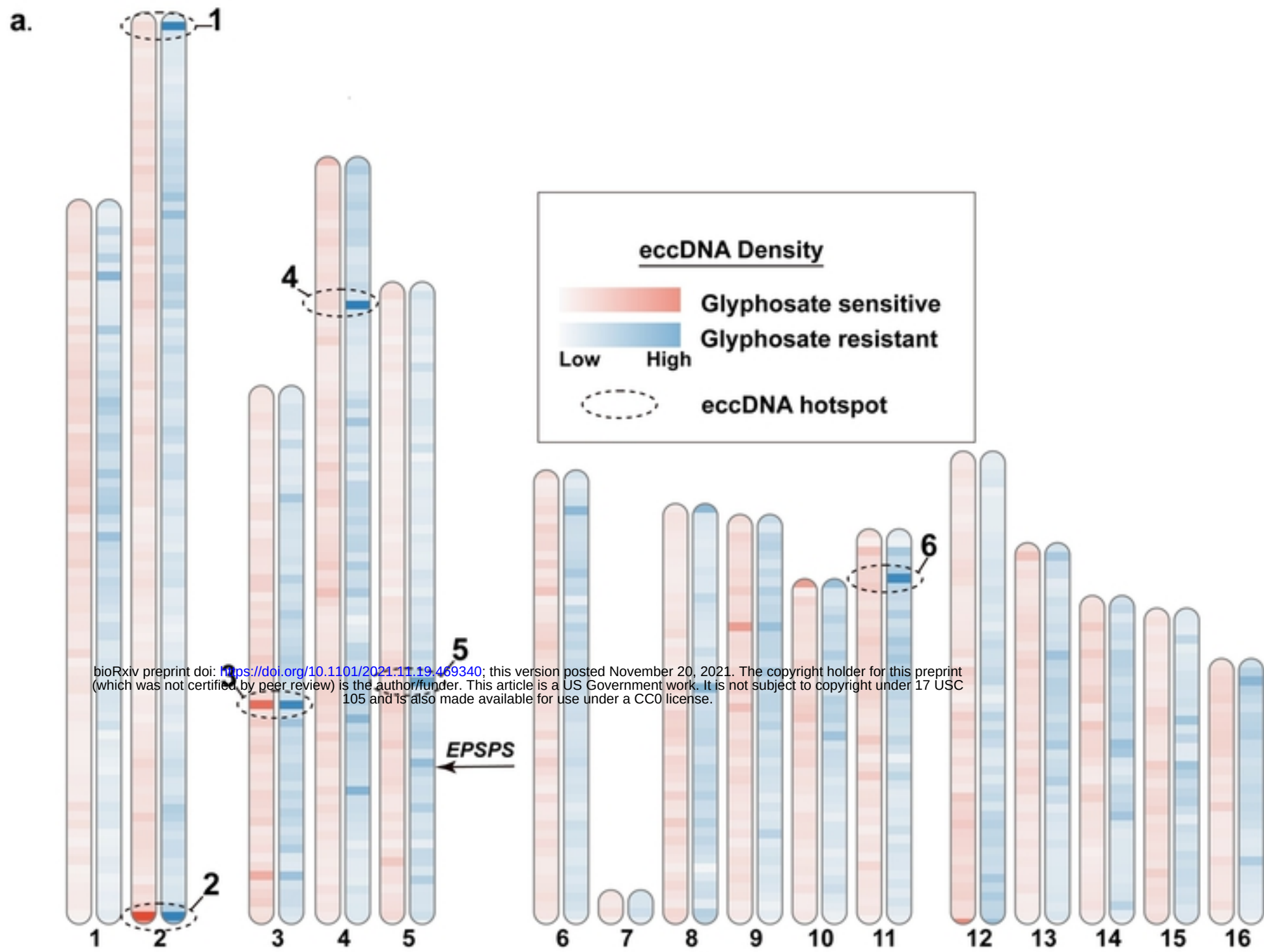

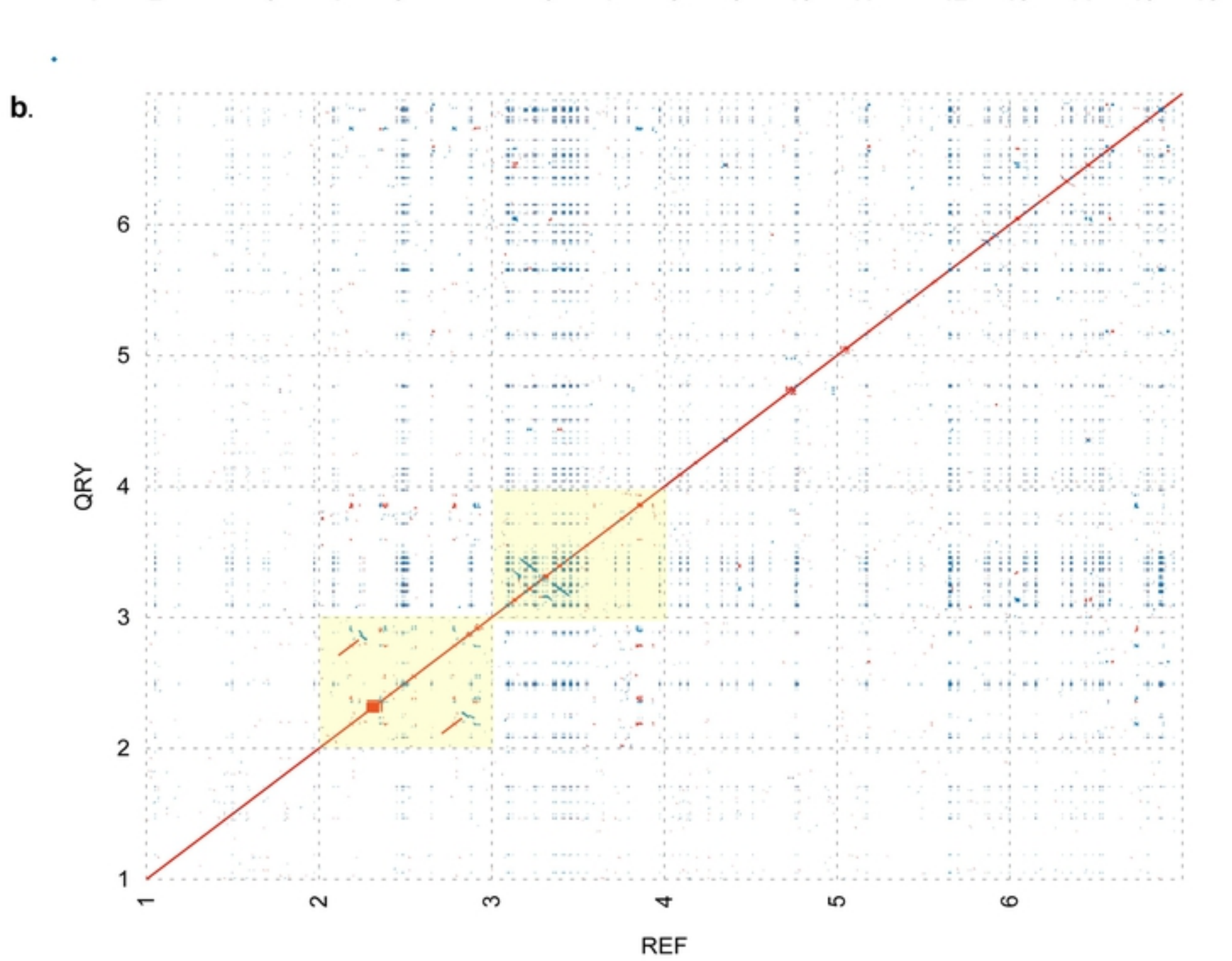

Fig 9